Electronic Supplementary Information for

Rotational Dynamics of Organic Cations in $CH_3NH_3PbI_3$ Perovskite

Tianran Chen, Benjamin J. Foley, Bahar Ipek, Madhusudan Tyagi, John R. D. Copley, Craig M. Brown, Joshua J. Choi*, Seung-Hun Lee*

*Corresponding authors. E-mail: shlee@virginia.edu, jjc6z@virginia.edu

Neutron Diffraction Data and Crystal Structure Refinement

Fig. S1 (a) shows the neutron diffraction data taken at 4 K. The Bragg peaks were fitted using the Rietveld refinement method to determine the crystal structure at 5 K, using GSAS (*S1*) package along with EXPGUI (graphical user interface) (*S2*). The refined crystal structure with an orthorhombic $Pnma$ space group was the same as that reported by Baikie *et al*. (*S3*) and Stoumpos *et al*. (*S4*) The structural parameters are listed in Table S1 and the resulting crystal structure is plotted in Fig. S1.

Table S1. Crystal structural parameters of $CH_3NH_3PbI_3$ for 4 K. Positions within orthorhombic space group $\boldsymbol{Pnma}$ and occupancies per a chemical unit cell (c.u.) in $CH_3NH_3PbI_3$ at $\boldsymbol{T = 4}$ K as determined by Rietveld analysis of the neutron diffraction data shown in Fig. S1 using the GSAS. The lattice parameters are a = 8.8155(4) Å, b = 12.5980(6) Å, and c = 8.5637(5) Å. Isotropic Debye-Waller factors, $\mathbf{exp}\left(-\langle \boldsymbol{u}^2\rangle \boldsymbol{Q}^2\right)$, were used where $\langle \boldsymbol{u}^2\rangle$ is the mean squared displacement. The resulting overall reduced $\boldsymbol{\chi^2 = 1.089}$.

Site	$\boldsymbol{x}$	$\boldsymbol{y}$	$\boldsymbol{z}$	$\boldsymbol{n}$/c.u.	$\sqrt{\langle \boldsymbol{u}^2\rangle}$/Å
Pb	1/2	0	0	4	0.0095(9)
I1	0.4844(11)	1/4	-0.0531(10)	4	0.0094(17)
I2	0.1871(6)	0.0165(5)	0.1818(6)	8	0.0078(11)
N	0.9390(6)	3/4	0.0294(6)	4	0.0127(11)
C	0.9166(9)	1/4	0.0683(10)	4	0.0200(20)
H1	0.3536(14)	0.1785(8)	0.4603(17)	8	0.0386(32)
H2	0.6305(10)	0.1877(7)	0.4983(14)	8	0.0172(22)
H3	0.5506(28)	1/4	0.6524(14)	4	0.0370(46)
H4	0.4601(37)	1/4	0.3159(19)	4	0.0635(62)

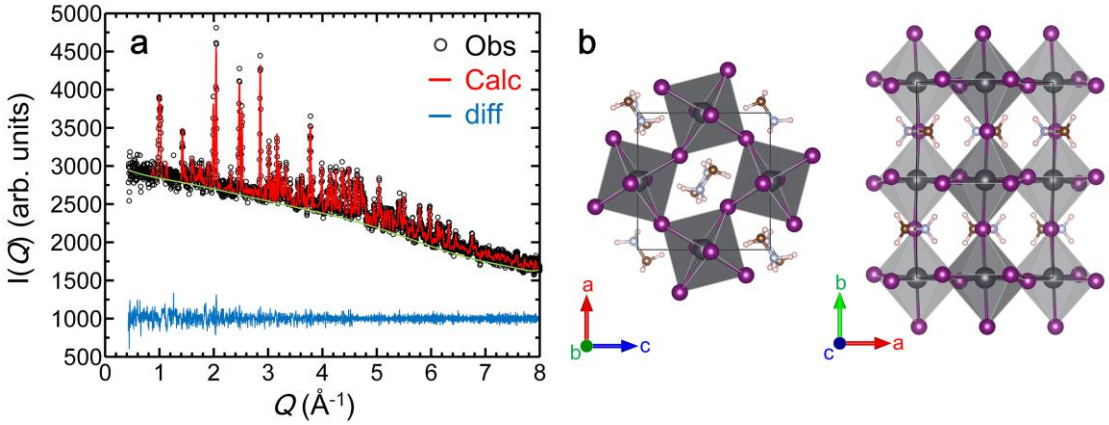

Fig. S1 (**a**) Neutron diffraction data collected for $CH_3NH_3PbI_3$ sample at 4 K. (**b**) The crystal structure determined by Rietveld refinement of the NPD data. The structural parameters are listed in Table S1. Note that in the orthorhombic space group $Pnma$, the longest axis is chosen to be *b*-axis (*b* = 12.5980(6) Å), while in the tetragonal space group $I4/mcm$, the long axis is chosen to be *c*-axis (*c* = 12.5944(7) Å) in the literature (*S3-5*).

DCS Data from $CH_3NH_3PbI_3$ and $CsPbI_3$

Fig. S2 shows DCS data obtained from the powder samples of $CH_3NH_3PbI_3$ and $CsPbI_3$ at 300 K. As shown in Fig. S2 (a), $CH_3NH_3PbI_3$ exhibits strong quasi-elastic scattering at 300 K that is extended up to a few meV and is broad in Q. On the other hand, the strong quasi-elastic scattering is absent in $CsPbI_3$ at 300 K. Thus we conclude that the quasi-elastic scattering present in $MAPbI_3$ comes from motions of the $CH_3NH_3^+$, which is confirmed by our analysis described in the text.

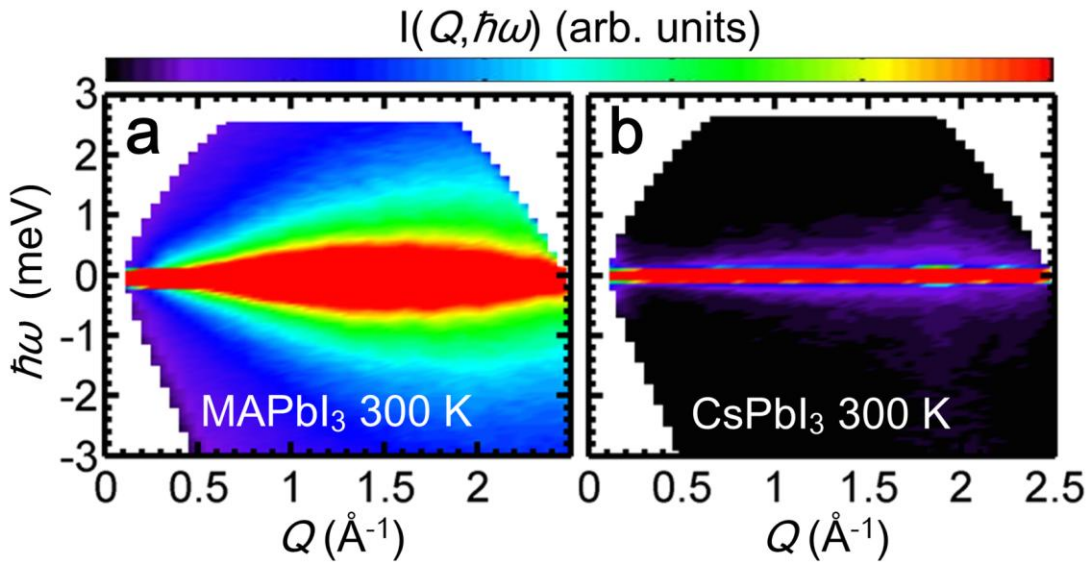

Fig. S2. Contour maps of quasi-elastic neutron scattering data taken from $CH_3NH_3PbI_3$ and $CsPbI_3$ at 300K at DCS $(\lambda = 4.8\ \text{Å})$.

Jump Models for $CH_3NH_3PbI_3$

(This section is in the main text but is repeated here for reader convenience.)

The rotation model that accounts for the existence of a preferential orientation is called a 'jump model'. (*S6*) Since the $CH_3NH_3^+$ molecule is located inside the cuboctahedral cage, its rotational motions are restricted by its own symmetry as well as by the local crystal symmetry of the cage. The possible rotational modes can be accounted for by the irreducible representations of the direct product of the symmetry of the local crystal environment ($\boldsymbol{C}$) and that of the molecule ($\boldsymbol{M}$); $\boldsymbol{\Gamma} = \boldsymbol{C} \otimes \boldsymbol{M}$. Here we consider proper rotations only and do not consider improper rotations such as inversion and mirror reflection. Since this group theory has been extensively described in many textbooks including Ref. (*S6*), we will state here only the basic formalism that is necessary for our discussion. In the group theory, the static and dynamic structure factor for rotational motions of molecules embedded in a crystal can be written as (*S6*)

$$S(Q,\hbar\omega) = e^{-\langle u^2\rangle Q^2}\left(\sum_{\gamma} A_{\gamma}(Q)\frac{1}{\pi}\frac{\tau_{\gamma}}{1+\omega^2\tau_{\gamma}^2}\right) \qquad \text{(S1)}$$

where the sum over γ runs over all the irreducible representations of $\boldsymbol{\Gamma}$, $\boldsymbol{\Gamma}_\gamma$. For a polycrystalline sample, $A_\gamma(Q)$ is given by (*S6*)

$$A_\gamma(Q) = \frac{l_\gamma}{g}\sum_\alpha\sum_\beta \chi_\gamma^{\alpha\beta}\sum_{C_\alpha}\sum_{M_\beta} j_0\left(Q\left|\boldsymbol{R} - C_\alpha M_\beta \boldsymbol{R}\right|\right) \qquad \text{(S2)}$$

Here g is the order of $\boldsymbol{\Gamma}$ and l_γ is the dimensionality of $\boldsymbol{\Gamma}_\gamma$. The sums over α and β run over all the classes of $\boldsymbol{C}$ and $\boldsymbol{M}$, respectively, and the sums over C_α and M_β run over all the rotations that belong to the crystal class, α, and to the molecule class, β, respectively. The characters of $\boldsymbol{\Gamma}_\gamma$, $\chi_\gamma^{\alpha\beta}$, are the products of the products of the characters of $\boldsymbol{C}_{\gamma_C}$ and $\boldsymbol{M}_{\gamma_M}$, $\chi_{\gamma_C}^{\alpha}$ and $\chi_{\gamma_M}^{\beta}$, respectively; $\chi_\gamma^{\alpha\beta} = \chi_{\gamma_C}^{\alpha}\chi_{\gamma_M}^{\beta}$. $j_0(x)$ is the zeroth spherical Bessel function and, $\left|\boldsymbol{R} - C_\alpha M_\beta \boldsymbol{R}\right|$, called the jump distance, is the distance between the initial atom position $\boldsymbol{R}$, and final atom position $C_\alpha M_\beta \boldsymbol{R}$. The relaxation time for the $\boldsymbol{\Gamma}_\gamma$ mode, τ_γ, can be written in terms of the relaxation times for $\boldsymbol{C}_\alpha$ and $\boldsymbol{M}_\beta$, τ_α and τ_β, respectively, (*S6*)

$$\frac{1}{\tau_\gamma} = \sum_\alpha \frac{n_\alpha}{\tau_\alpha}\left(1 - \frac{\chi_\gamma^{\alpha e}}{\chi_\gamma^{Ee}}\right) + \sum_\beta \frac{n_\beta}{\tau_\beta}\left(1 - \frac{\chi_\gamma^{E\beta}}{\chi_\gamma^{Ee}}\right) \qquad \text{(S3)}$$

where n_α and n_β are the number of symmetry rotations that belong to the classes, α and β, respectively. E and e represent the identity operations of $\mathbf{C}$ and $\mathbf{M}$, respectively**.**

.

$\boldsymbol{\Gamma} = \boldsymbol{C_4} \otimes \boldsymbol{C_3}$ Jump Model

In this model, the local crystal environment has a four-fold symmetry and the molecule itself has a three-fold rotational symmetry as the $CH_3NH_3^+$ does in the tetragonal phase (see Fig. S3). The character tables for the irreducible representations of the $\boldsymbol{C_4}$ and $\boldsymbol{C_3}$ point groups are shown in Table S2.

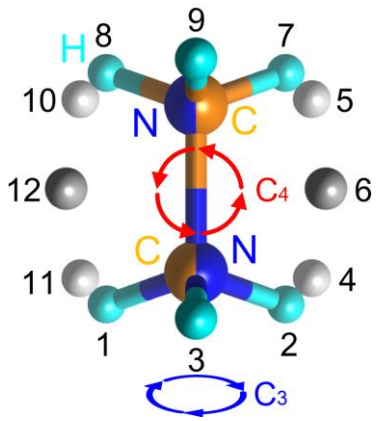

Fig. S3. The $CH_3NH_3^+$ in the tetragonal environment. The small spheres in sky blue and their counter parts in grey, representing 12 crystallographically equivalent sites for hydrogen atoms in the initial orientation and upon rotation of the molecular axis by 90°, respectively. Since the motions of the two halves of the $CH_3NH_3^+$ ion can be treated independently in the jump model calculations, the H atoms attached to C and N are plotted in an eclipsed configuration rather than the staggered configuration shown in Fig. S4, to clearly show the jump distances.

Table S2. The $\boldsymbol{C_4}$ point group has three classes and three irreducible representations, two one-dimensional (*A* and *B*) and one two-dimensional (*E*) representations. The $\boldsymbol{C_3}$ point group has two classes and two irreducible representations, a one-dimensional (*A*) and one two-dimensional (*E*) representations.

C = C$_4$	E	$2C_4$	C_2
A	1	1	1
B	1	-1	1
E	2	0	-2

M = C$_3$	E	$2C_3$
A	1	1
E	2	-1

The resulting point group for the possible rotational motions, $\boldsymbol{\Gamma}$, has 6 irreducible representations: $\boldsymbol{\Gamma_\gamma} = \{\boldsymbol{A\otimes A}, \boldsymbol{A\otimes E}, \boldsymbol{B\otimes A}, \boldsymbol{B\otimes E}, \boldsymbol{E\otimes A}, \boldsymbol{E\otimes E}\}$. It is straightforward to get correlation times from Eq. S3;

$$\frac{1}{\tau_{\boldsymbol{A\otimes A}}} = 0, \frac{1}{\tau_{\boldsymbol{A\otimes E}}} = \frac{3}{\tau_{\boldsymbol{C_3}}}, \frac{1}{\tau_{\boldsymbol{B\otimes A}}} = \frac{4}{\tau_{\boldsymbol{C_4}}},$$

$$\frac{1}{\tau_{\boldsymbol{B\otimes E}}} = \frac{4}{\tau_{\boldsymbol{C_4}}} + \frac{3}{\tau_{\boldsymbol{C_3}}}, \frac{1}{\tau_{\boldsymbol{E\otimes A}}} = \frac{4}{\tau_{\boldsymbol{C_4}}} + \frac{2}{\tau_{\boldsymbol{C_2}}}, \frac{1}{\tau_{\boldsymbol{E\otimes E}}} = \frac{2}{\tau_{\boldsymbol{C_4}}} + \frac{2}{\tau_{\boldsymbol{C_2}}} + \frac{3}{\tau_{\boldsymbol{C_3}}},$$

Now let us calculate $A_\gamma(Q)$ for $\boldsymbol{\Gamma} = \boldsymbol{C_4} \otimes \boldsymbol{C_3}$. First, we need to know how a hydrogen atom moves from one to another crystallographically equivalent site under the combined symmetry operations of the two point groups of $\boldsymbol{C} = \boldsymbol{C_4}$ and $\boldsymbol{M} = \boldsymbol{C_3}$. Table S4 lists the geometrical information.

Table S4. Geometrical information for a hydrogen atom moving from one site to another equivalent site under the combined symmetry operations of the two point groups of $\boldsymbol{C} = \boldsymbol{C_4}$ and $\boldsymbol{M} = \boldsymbol{C_3}$. The resulting jump distances r_i are, using the notation $R_{i,j} = |\boldsymbol{R}_i - \boldsymbol{R}_j|$, $r_1 = R_{1,2}$, $r_2 = R_{1,4}$, $r_3 = R_{1,5}$, $r_4 = R_{1,7}$, $r_5 = R_{1,8}$, $r_6 = R_{1,11}$, $r_7 = R_{1,6}$, $r_8 = R_{1,9}$, $r_9 = R_{1,12}$, $r_{10} = R_{3,6}$ where $\boldsymbol{R}_i$ is the position of the *i*th hydrogen atom numbered as in Fig. S3.

Initial positions		Final positions			Jump Distance		
		E	C_3	C_3^2	E	C_3	C_3^2
1	E	1	2	3	0	r_1	r_1
	C_4	4	5	6	r_2	r_3	r_7
	C_2	7	8	9	r_4	r_5	r_8
	C_4^3	10	11	12	r_2	r_6	r_9
2	E	2	3	1	0	r_1	r_1
	C_4	5	6	4	r_2	r_3	r_7
	C_2	8	9	7	r_4	r_5	r_8
	C_4^3	11	12	10	r_2	r_6	r_9
3	E	3	1	2	0	r_1	r_1
	C_4	6	4	5	r_{10}	r_9	r_7
	C_2	9	7	8	r_5	r_8	r_8
	C_4^3	12	10	11	r_{10}	r_9	r_7

$r_1 = R_{1,2}$
$r_2 = R_{1,4}$
$r_3 = R_{1,5}$
$r_4 = R_{1,7}$
$r_5 = R_{1,8}$
$r_6 = R_{1,11}$
$r_7 = R_{1,6}$
$r_8 = R_{1,9}$
$r_9 = R_{1,12}$
$r_{10} = R_{3,6}$

We can now calculate $A_\gamma(Q)$ using Eq. S3:

$$A_{\boldsymbol{A}\otimes\boldsymbol{A}}(Q) = \frac{1}{36}[3 + 6j_1 + 4j_2 + 2j_3 + 2j_4 + 3j_5 + 2j_6 + 4j_7 + 4j_8 + 4j_9 + 2j_{10}]$$

$$A_{\boldsymbol{A}\otimes\boldsymbol{E}}(Q) = \frac{1}{36}[6 - 6j_1 + 8j_2 - 2j_3 + 4j_4 - 2j_6 - 4j_7 - 4j_8 - 4j_9 + 4j_{10}]$$

$$A_{\boldsymbol{B}\otimes\boldsymbol{A}}(Q) = \frac{1}{36}[3 + 6j_1 - 4j_2 - 2j_3 + 2j_4 + 3j_5 - 2j_6 - 4j_7 + 4j_8 - 4j_9 - 2j_{10}]$$

$$A_{\boldsymbol{B}\otimes\boldsymbol{E}}(Q) = \frac{1}{36}[6 - 6j_1 - 8j_2 + 2j_3 + 4j_4 + 2j_6 + 4j_7 - 4j_8 + 4j_9 - 4j_{10}]$$

$$A_{\boldsymbol{E}\otimes\boldsymbol{A}}(Q) = \frac{1}{36}[6 + 12j_1 - 4j_4 - 6j_5 - 8j_8]$$

$$A_{\boldsymbol{E}\otimes\boldsymbol{E}}(Q) = \frac{1}{36}[12 - 12j_1 - 8j_4 + 8j_8]$$

where $j_i = j_0(Qr_i)$ is the zeroth spherical Bessel function.

The elastic and quasielastic incoherent structure factors, $A_\gamma(Q)$, are plotted in Fig. S4. Atomic positions of $CH_3NH_3^+$ are obtained from our refinement of 4 K neutron diffraction data.

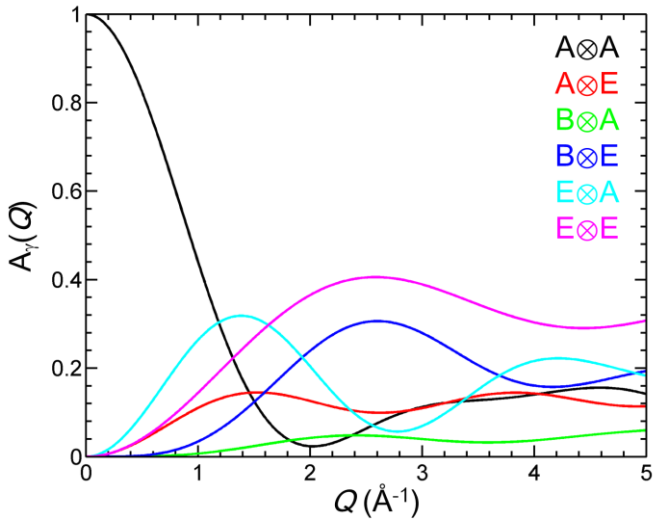

Fig. S4. *Q*-dependences of the calculated elastic and quasi-elastic incoherent structure factors for the $\boldsymbol{C_4 \otimes C_3}$ jump model. The irreducible representation A⊗A gives elastic contribution $\left(\frac{1}{\tau_{A\otimes A}} = 0\right)$ while the rest give quasi-elastic contributions.

$\boldsymbol{\Gamma = E \otimes C_3 = C_3}$ Jump Model

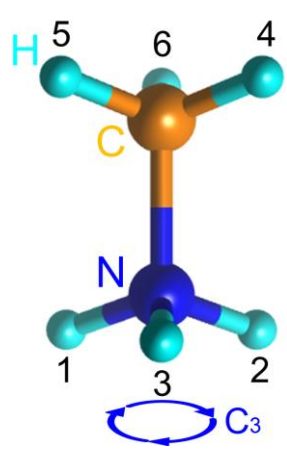

Fig. S5. $CH_3NH_3^+$ in the orthorhombic environment.

In this model, the orientation of the $CH_3NH_3^+$ is fixed due to hydrogen bonding between the NH_3 and iodide atoms. Thus $\boldsymbol{C} = \boldsymbol{E}$, and $\boldsymbol{\Gamma} = \boldsymbol{E} \otimes \boldsymbol{C_3} = \boldsymbol{C_3}$. The character table of the point group $\boldsymbol{C_3}$ is:

$\boldsymbol{\Gamma} = \mathbf{C_3}$	E	$2C_3$
A	1	1
E	2	-1

The correlation times can be obtained by,

$$\frac{1}{\tau_\gamma} = \sum_\alpha \frac{n_\alpha}{\tau_\alpha}\left(1 - \frac{\chi_\gamma^\alpha}{\chi_\gamma^E}\right) \qquad \text{(S4)}$$

It is straightforward to calculate the equation to get

$$\frac{1}{\tau_{\boldsymbol{A}}} = 0, \frac{1}{\tau_{\boldsymbol{E}}} = \frac{3}{\tau_{\boldsymbol{C_3}}}$$

The elastic and quasi-elastic incoherent structure factors can be obtained by

$$A_\gamma(Q) = \frac{\chi_\gamma^E}{g}\sum_\alpha \chi_\gamma^\alpha \sum_{\Gamma_\alpha} j_0(Q|\boldsymbol{R} - \Gamma_\alpha \boldsymbol{R}|) \qquad \text{(S5)}$$

The jump distance of the three-fold rotation is $r = |\boldsymbol{R}_1 - \boldsymbol{R}_2|$, where $\boldsymbol{R}_i$ is the position of the *i*th H atom numbered as in Fig. S4. Thus, $A_\gamma(Q)$ becomes

$$A_{\boldsymbol{A}}(Q) = \frac{1}{3}[1 + 2j_0(Qr)]$$

$$A_{\boldsymbol{E}}(Q) = \frac{2}{3}[1 - j_0(Qr)]$$

The elastic and quasi-elastic incoherent structure factors, $A_\gamma(Q)$, are plotted as a function of Q in Fig. S6.

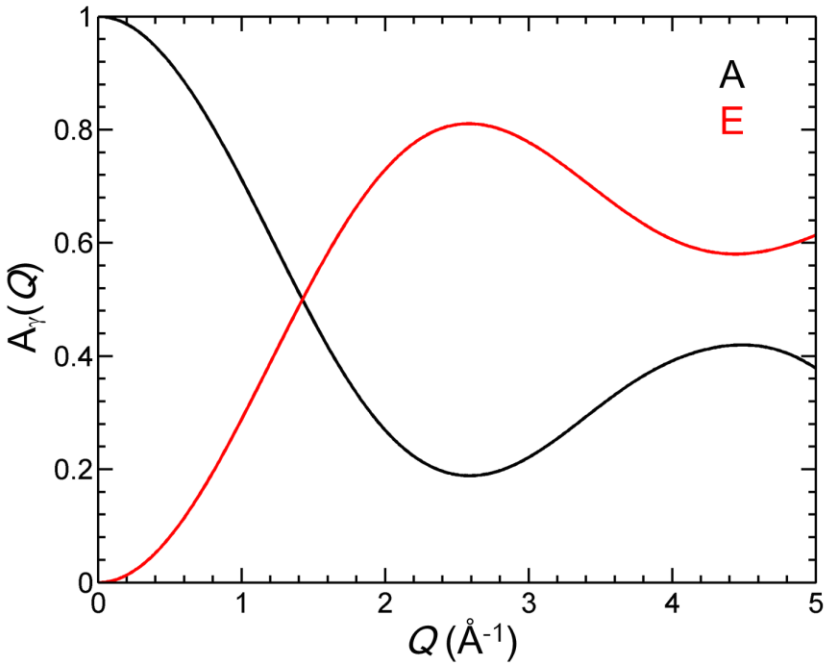

Fig. S6. Q-dependences of the calculated elastic and quasi-elastic incoherent structure factors for the $\boldsymbol{C_3}$ jump model. The irreducible representation A gives elastic contribution $\left(\frac{1}{\tau_{A\otimes A}} = 0\right)$ while E gives quasi-elastic contribution.

C3 jump distances in CH3 and NH3 groups

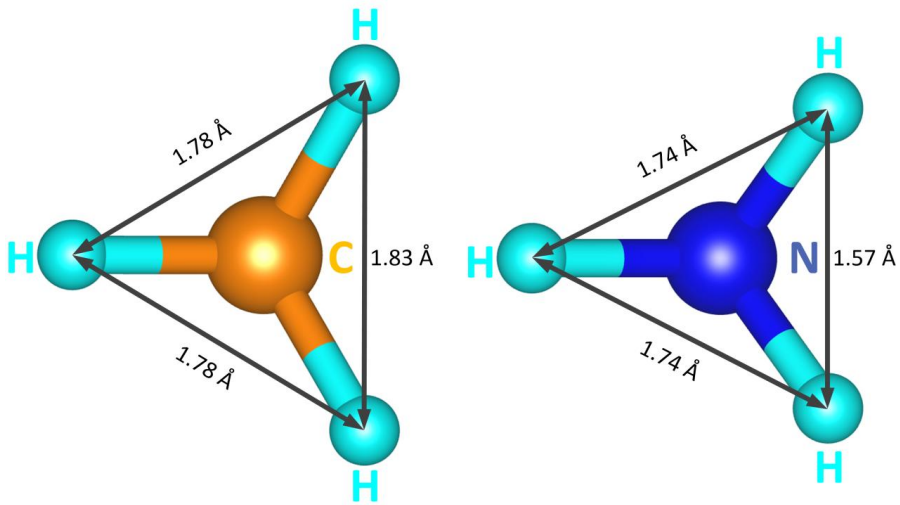

Fig. S7. C_3 Jump distances determined by refinement of 4K neutron powder diffraction data

As shown in Fig. S7, the average C_3 jump distance of CH_3, r_1, is about 7% larger than that of NH_3, r_2. In all of our calculations, we used the average jump distance, $\bar{r} = \frac{r_1+r_2}{2}$. Then, r_1 and r_2 can be written as $r_1 = \bar{r} + \Delta, r_2 = \bar{r} - \Delta$, where $\frac{\Delta}{\bar{r}} \approx 3\%$. The Q-dependence of $S(Q, \hbar\omega)$ has a functional form of the lth spherical Bessel function, $j_l(Qr)$. The difference between using two separate jump distances, r_1 and r_2, and using the average jump distance, $\bar{r}$, is minimal:

$$j_l(Q\bar{r}) - \frac{j_l\big(Q(\bar{r}+\Delta)\big) + j_l\big(Q(\bar{r}-\Delta)\big)}{2} \approx \frac{1}{2} j_l''(Q\bar{r}) Q^2 \Delta^2$$

Since $\left(\frac{\Delta}{\bar{r}}\right)^2 \approx 0.1\%$, the effect of the difference is negligible within our experimental uncertainty.

References

(*S1*) A. C. Larson and R. B. Von Dreele, Los Alamos National Laboratory, 1994; pp. 86–748.
(*S2*) B. H. Toby, *J. Appl. Crystallogr.* 2001, 34, 210–213.
(*S3*) T. Baikie, Y. Fang, J. M. Kadro, M. Schreyer, F. Wei, S. G. Mhaisalkar, M. Gratzel and T. J. White, *J. Mater. Chem. A* 2013, 1, 5628.
(*S4*) C. C. Stoumpos, C. D. Malliakas and M. G. Kanatzidis, *Inorg. Chem.* 2013, 52, 9019–9038.
(*S5*) M. T. Weller, P. Henry, O. Weber, A. Di Pumpo and T. Hansen, *Chem. Commun.*,

2015, DOI: 10.1039/C4CC09944C.
(*S6*) M. Bee´, *Quasielastic Neutron Scattering* (Adam Hilger, Bristol, 1988).
(*S7*) Certain commercial equipment, instruments, or materials are identified in this paper to foster understanding. Such identification does not imply recommendation or endorsement by the National Institute of Standards and Technology, nor does it imply that the materials or equipment identified are necessarily the best available for the purpose.